

Modeling Multi-Cellular Dynamics Regulated by ECM-Mediated Mechanical Communication via Active Particles with Polarized Effective Attraction

Yu Zheng*,¹ Qihui Fan*,^{2,3} Christopher Z. Eddy,⁴ Xiaochen Wang,^{2,3} Bo Sun,^{4,†} Fangfu Ye,^{2,3,‡} and Yang Jiao^{5,1,§}

¹*Department of Physics, Arizona State University, Tempe, AZ 85287*

²*Beijing National Laboratory for Condensed Matter Physics and CAS Key Laboratory of Soft Matter Physics, Institute of Physics, Chinese Academy of Sciences, Beijing 100190, China*

³*School of Physical Sciences, University of Chinese Academy of Sciences, Beijing 100049, China*

⁴*Department of Physics, Oregon State University, Corvallis, OR 97331*

⁵*Materials Science and Engineering, Arizona State University, Tempe, AZ 85287*

Collective cell migration is crucial to many physiological and pathological processes such as embryo development, wound healing, and cancer invasion. Recent experimental studies have indicated that the active traction forces generated by migrating cells in fibrous extracellular matrix (ECM) can mechanically remodel the ECM, giving rise to bundle-like meso-structures bridging individual cells. Such fiber bundles also enable long-range propagation of cellular forces, leading to correlated migration dynamics regulated by the mechanical communication among the cells. Motivated by these experimental discoveries, we develop an active-particle model with polarized effective attractions (APPA) for modeling emergent multi-cellular migration dynamics regulated by ECM-mediated mechanical communications. In particular, the APPA model generalizes the classic active-Brownian-particle (ABP) model by imposing a pairwise polarized attractive force between the particles, which depends on the instantaneous dynamic states of the particles and mimics the effective mutual pulling between the cells via the fiber bundle bridge. Active particles with polarized pairwise attractions exhibit enhanced aggregation behaviors compared to classic active Brownian particles, especially at lower particle densities and larger rotational diffusivities. Importantly, in contrast to the classic ABP system where the particle velocities are not correlated for all particle densities, the high-density phase of APPA system exhibits strong dynamic correlation, which is characterized by the slowly decaying velocity correlation functions with a correlation length comparable to the linear size of high-density phase domain (i.e., cluster of the particles). The strongly correlated multi-cellular dynamics predicted by the APPA model are subsequently verified in *in vitro* experiments using MCF-10A cells. Our studies also indicate the importance of incorporating ECM-mediated mechanical coupling among the migrating cells for appropriately modeling emergent multi-cellular dynamics in complex micro-environments.

I. INTRODUCTION

Cell migration in complex extracellular matrix (ECM), a complex dynamic process involving a series of intra-cellular and extra-cellular activities [1, 2], is crucial to many physiological and pathological processes including tissue regeneration, immune response and cancer progression [3–6]. It has been well established that cell migration can be significantly influenced by the micro-environment via chemotaxis [7], durotaxis [8–10], haptotaxis [11], and contact guidance [12–14]. Migrating cells can generate active pulling forces via actomyosin contraction [15–17], which are transmitted to the ECM fibers through focal adhesion complexes [18–20]. Such active forces mechanically remodel the local ECM, e.g., by re-orienting the collagen fibers, forming fiber bundles and increasing the local stiffness of ECM [21–27]. Recent studies have indicated that a delicate balance among the magnitude of the pulling forces, the cell-ECM adhesion strength, and

the ECM rigidity is required to achieve an optimal mode of single cell migration [28].

In a multi-cellular system, the active pulling forces generated by individual cells can propagate in the ECM and can be sensed by distant cells [29–39]. This ECM-mediated mechanical coupling among the cells could further influence the migration of the individual cells, which in turn alters the ECM structure and properties, leading to a rich spectrum of collective migratory behaviors [36]. For example, a recent *in vitro* experimental study [40] showed that highly motile MCF-10A cells migrating on thick layer of collagen-I gel develop strongly correlated dynamics via mechanically remodeled fiber bundles bridging the migrating cells (see Fig. 1). In addition, it was shown via laser ablation techniques that the fiber bundles carry significant tensile forces, and thus strongly suggesting the observed collective migration dynamics was resulted from the mechanical communications among the cells via the remodeled fiber bundles [38].

Many computational models have been developed to investigate the individual and multi-cellular migration dynamics [41–43] as well as various sub-cellular processes involved in cell migration [44–49]. Examples include vertex-based models [52], multi-state cellular Potts models [53], cellular automaton models [54–57]. Recently, the influences of the cell-ECM interactions and/or ECM-

*These authors contributed equally to this work.

†correspondence sent to: sunb@physics.oregonstate.edu

‡correspondence sent to: fye@iphy.ac.cn

§correspondence sent to: yang.jiao.2@asu.edu

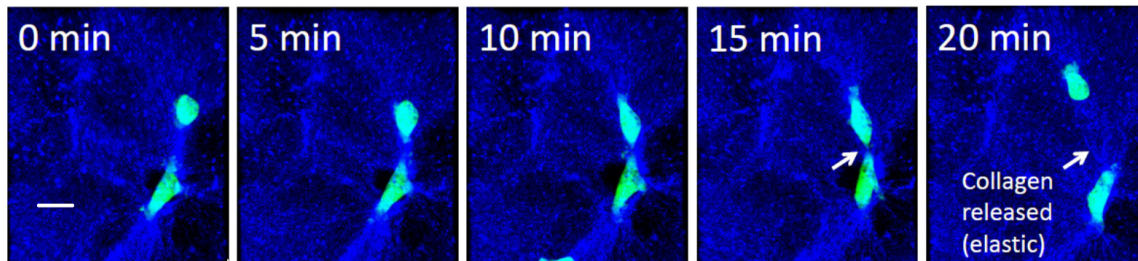


FIG. 1: Confocal microscopy images showing strongly correlated migration of a pair of MCF-10A cells on thick collagen gel ($\sim 2mm$) [40]. The scale bar is $30 \mu m$. The contraction of the cells at the front edge mechanically remodel the ECM, leading to the formation of fiber bundles bridging the migrating cells. It has been shown via laser ablation techniques that the fiber bundles carry significant tensile forces, and thus strongly suggesting the observed collective migration dynamics was resulted from the mechanical communications among the cells via the remodeled fiber bundles.

mediated indirect cell-cell interactions on individual and collective migration dynamics are started to be explicitly considered and incorporated in cell migration models [58–69].

The active-particle model is one of most widely used model for multi-cellular dynamics. In the seminal work of Vicsek and colleagues [50], it was shown that local velocity correlation among neighboring active particles can induce dynamic phase transition in the system. The Vicsek model was subsequently generalized to include cell-cell contact interactions to investigate collective cellular dynamics such as cell sorting [70]. More recently, the active Brownian particle model (and its different variants) have received intensive attentions. In these models, a migrating cell is treated as an “active particle” whose dynamics is mainly determined by an active self-propelling force, a random drift and various effective particle-particle and/or particle-environment interactions [71–73]. A wide spectrum of collective dynamics have been observed and investigated in active-particle systems [51].

In this work, motivated by the experimental observation that active pulling forces generated by migrating cells and propagated via fiber bundles can lead to strongly correlated migration dynamics (e.g., nearby cells effectively attract each other and move towards each other, see Fig. 1), we develop an active-particle model with polarized effective attractions (APPA) for modeling emergent multi-cellular migration dynamics regulated by ECM-mediated mechanical communications. The APPA model generalizes the classic active-Brownian-particle (ABP) model by imposing a pairwise polarized attractive force between the migrating cells (modeled as active particles), which depends on the instantaneous dynamic states of cells including the position and velocity alignment and mimics the effective mutual pulling between the cells via the fiber bundle bridge.

The APPA model predicts enhanced aggregation behaviors compared to those predicted by the classic ABP model, especially at lower particle densities ϕ (i.e., the fraction of space covered by the particles) and larger ro-

tational diffusivities D_r of the persistent cellular velocity. Importantly, in contrast to the classic ABP system where the particle velocities are not correlated for all ϕ , the high-density phase of APPA system (i.e., densely packed aggregates of the particles) exhibits strong dynamic correlation, which is revealed by the velocity vector map and characterized by the slowly decaying velocity correlation functions with a correlation length comparable to the linear size of high-density particle aggregate. The strongly correlated multi-cellular dynamics predicted by the APPA model are subsequently verified in *in vitro* experiments observing MCF-10A cells migrating on 3D collagen gels, which exhibit strongly correlated migration dynamics at high cellular densities. These results indicate the importance of incorporating ECM-mediated mechanical coupling among the migrating cells for appropriately modeling emergent multi-cellular dynamics in complex micro-environments.

II. METHODS

A. Active Brownian particle model for single cell migration

Before describing the details of the active particle model with polarized effective attractions (APPA) developed here, we first briefly introduce the classic active Brownian particle (ABP) model for single cell migration simulations and its biophysical background. More details and applications of the ABP model and its generalizations can be found in recent reviews, e.g., Ref.[51]. We note that cell migration in fibrous extracellular matrix (ECM) is a complex dynamic process involving a series of intra-cellular and extra-cellular activities including the development of membrane protrusions, formation of focal adhesion sites, locomotion due to actin filament contraction, and detachment of the rear end [1, 2]. In general, the migration dynamics can be significantly influenced by the heterogeneity of local ECM microstructure [74, 75] and mechanical properties [22, 28, 35, 77–82].

In a statistically homogeneous ECM (e.g., one with uniform collagen density and random fiber orientations), a migrating cell can be very well modeled as an active Brownian particle, whose dynamics follows the over-damped Langevin equation, i.e.,

$$\dot{\mathbf{r}}_i(t) = v_0 \mathbf{e}_i + \sqrt{2D_t} \boldsymbol{\Gamma}_i(t) \quad (1)$$

where the subscript i is the particle index, v_0 is the persistent speed of the particle, \mathbf{e}_i is a unitary vector characterizing the persistent speed direction and subject to rotational diffusion with diffusion coefficient D_r ; D_t is the translational diffusivity of the particle and $\boldsymbol{\Gamma}_i(t)$ is a white noise. The model parameters are determined by cell phenotype, ECM microenvironment, as well as stochastic subcellular processes such as actin polymerization, cell-ECM adhesion turn over. The small set of parameters is particularly attractive in understanding the complex, multi-scale processes for 3D cell migration.

The model parameters are determined by cell phenotype, ECM microenvironment, as well as stochastic subcellular processes such as actin polymerization, cell-ECM adhesion turn over. The small set of parameters is particularly attractive in understanding the complex, multi-scale processes for 3D cell migration.

B. Modelling effects of ECM-mediated mechanical coupling via polarized attraction

A migrating cell also generates active pulling forces [15–17], which are transmitted to the ECM fibers via focal adhesion complexes [18–20]. Such active forces remodel the local ECM, e.g., by re-orienting the collagen fibers, forming fiber bundles and increasing the local stiffness of ECM [21–27]. Importantly, the remodeled fiber bundles can efficiently transmit the active (pulling) forces generated by the cells, enabling mechanical dialogs between the migrating cells.

As illustrated in Fig. 1, the fiber bundles typically formed between two migrating cells, connecting the polarized pulling ends of the cells. This allows the pulling forces generate by one cell to propagate to and sensed by the other cell, and vice versa. Therefore, we model the effects of this mechanical dialog here using effective attraction between the cells. Since cell velocity is typically aligned with the polarization direction, the effective attraction is also polarized (instead of being isotropic). We also note that the fiber bundles disappear as the cell polarization direction changes, e.g., when the two cells are moving away from one another (see Fig. 1). This suggests that the fiber bundles, the structural support for the effective attractions between the cells, are mainly due to elastic ECM remodeling and temporary [39, 40]. Therefore, in our model, we consider the polarized effective attraction only exist between a pair of migrating cells that are moving *towards* each other (see the mathematical details below). The underlying ECM network and the

remodeled fiber bundles will not be explicitly considered in our model.

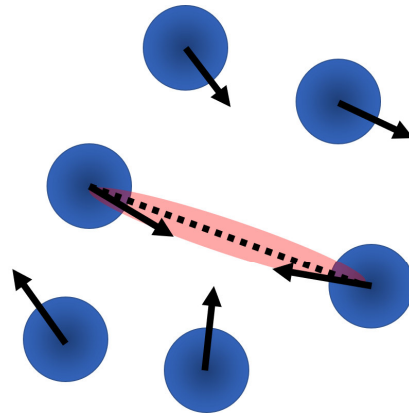


FIG. 2: Schematic illustration of the effective polarized attraction between two migrating cells, which depends on both the positions and velocities of the cells. Specifically, the effective attraction is non-zero only when the two cells are moving towards one another (i.e., with the velocities anti-parallel aligned within a prescribed tolerance).

Specifically, we consider the dynamics of active particles with polarized effective attractions are described by the generalized over-damped Langevin equation, i.e.,

$$\dot{\mathbf{r}}_i(t) = v_0 \mathbf{e}_i + \mu \mathbf{F}_i^{ECM} + \sqrt{2D_t} \boldsymbol{\Gamma}_i(t) \quad (2)$$

where μ is the cellular motility and \mathbf{F}_i^{ECM} is the total force due to ECM-mediated mechanical coupling among migrating cells. The other parameters are the same as in Eq. (1). We also consider that each particle (cell) possesses a hard-core exclusion volume modeled as a hard sphere with radius R_c , which prevents the overlapping of the particles upon contact. The total force \mathbf{F}_i^{ECM} due to ECM-mediated mechanical coupling is given by

$$\mathbf{F}_i^{ECM} = \sum_j f_{ij}^a(r_{ij}, \dot{\mathbf{r}}_i, \dot{\mathbf{r}}_j) \quad (3)$$

where the sum is over all neighboring particles of particle i , and f_{ij}^a is the pair-wise polarized attraction between particles i and j , which depends on the particle separation distance r_{ij} as well as the dynamic state of the particles (i.e., $\dot{\mathbf{r}}_i, \dot{\mathbf{r}}_j$), i.e.,

$$f_{ij}^a(r_{ij}, \dot{\mathbf{r}}_i, \dot{\mathbf{r}}_j) = \begin{cases} \epsilon/r^\alpha, & r_{ij} > (R_i + R_j), \\ & \frac{\dot{\mathbf{r}}_i \cdot (\mathbf{r}_j - \mathbf{r}_i)}{|\dot{\mathbf{r}}_i| |\mathbf{r}_j - \mathbf{r}_i|} > 1 - \delta, \\ & \frac{\dot{\mathbf{r}}_j \cdot (\mathbf{r}_i - \mathbf{r}_j)}{|\dot{\mathbf{r}}_j| |\mathbf{r}_i - \mathbf{r}_j|} > 1 - \delta \\ 0, & \text{otherwise} \end{cases} \quad (4)$$

where the force parameter ϵ characterizes the strength of the effective polarized attraction, which mainly depends on the cell phenotype and ECM mechanical properties; R_i and R_j are respectively the radius of particles i and

j . δ is a threshold that quantifies the degree of anti-parallel alignment of the cell velocities, which is a necessary condition for ECM-mediated mechanical coupling. The exponent α in the power-law scaling $1/r^\alpha$ characterizes the propagation and decay of the active force in the ECM. We note that $\alpha = 1$ for an elastic continuum and recent studies indicate that the decay of active forces in ECM network can be slower (i.e., $\alpha < 1$) due to the unique “force chain” structures [35]. In our simulations, the exact value of α does not significantly influence the collective dynamics and we use $\alpha = 1$.

Eqs. (2)-(4) are employed in subsequent simulations of the active particles with polarized attractions (APPA). In particular, the particles are initially randomly placed in a periodic square simulation domain without overlapping. The initial velocities of particles are randomly oriented but the same magnitude v_0 . The particles are then evolved according to Eq. (2), where the velocities and positions of the particles are updated at discretized time steps dt . The updated velocity is re-scaled to v_0 while keeping its direction. The persistent direction of each particle is also updated by changing it by a small angle randomly selected from the interval $[-D_r, D_r]\pi$. Particle overlaps are removed by pushing each particle back by half of the overlapping distance along their center-center direction. The procedure is repeated until a prescribed number of time steps is achieved and the simulation is terminated.

C. Mean cluster size and velocity correlation function

We quantify the morphological evolution of the APPA systems using cluster statistics. Specifically, at a given time step, the particles are grouped into different clusters. We consider that two particles belong to the same cluster if the distance between their centers is less than a threshold (e.g., $d_{ij} < (R_i + R_j + \delta_d)$). We compute the *mean cluster size* [83–85] to quantify the degree of clustering/aggregation of the particles, i.e.,

$$S = \frac{\sum_{k=1}^{\infty} k^2 n_k}{\sum_{k=1}^{\infty} k n_k} \quad (5)$$

where k is number of particles that a cluster contains. A cluster containing k particles is called k -cluster. n_k is the probability that randomly selected cluster in the system is a k -cluster, which is computed by dividing the number of k -cluster by total number of clusters. It can be seen from Eq. (5) that $S \in [0, 1]$. A large S value (e.g., $S \sim 1$) indicates that the majority particles are contained in one (or a small number of) dominant clusters; while a small S value indicates that the particles in the system are scatters and the level of aggregation is low.

In addition, we employ the *velocity correlation function* to quantify the correlated particle dynamics on the two-

body (pair) level, i.e.,

$$C(r) = \left\langle \frac{\mathbf{u}_i \cdot \mathbf{u}_j}{|\mathbf{u}_i| |\mathbf{u}_j|} \right\rangle \quad (6)$$

where \mathbf{u} is the instantaneous particle velocities and $|\cdot|$ indicates the magnitude of the vector; r is the cell-center distance between a pair cells i and j ; the brackets $\langle \cdot \rangle$ indicates average over all cell pairs. Perfectly correlated pair dynamics is associated with $C(r) = 1$. This is the case when the velocities of all particles are perfectly aligned, e.g., indicating the cells are following one another during collective migration. On the other hand, $C(r) = -1$ is associated with anti-parallel velocities, i.e., when the cells are moving towards one another. $C(r) = 0$ indicates no correlations among the particles (migrating cells).

III. RESULTS

A. Enhanced aggregation and dynamic correlation due to long-range mechanical coupling

We employ the APPA model to investigate the collective dynamics of multi-cellular systems in homogeneous ECM. Examples of such systems include the *in vitro* experiments where non-metastatic MCF-10A cells migrate on 3D collagen gel. In this system, the strong motility of the MCF-10A cells can result in large active pulling forces, which propagate and influence the migration of other cells via the remodeled fiber bundles (see Fig. 1). To demonstrate the distinct dynamics resulted from the APPA model, in particular, the polarized effective attractions that mimics the mechanical dialogs between the cells, we also simulate the system using the classic ABP model. We use the following parameters in our simulations: $v_0 = 0.5 \mu\text{m}/\text{min}$, $\epsilon = 10nN/\mu\text{m}$, unless otherwise specified. In addition, we set the translational diffusivity $D_t = 0.01 \mu\text{m}^2/\text{min}$, which is small compared to the persistent speed. This is consistent with the experimental observation that MCF-10A cells on 3D collagen exhibit strong ballistic-like motions [40]. We note that the characteristic dynamics rising in the APPA systems are not sensitive to the exact values of these parameters.

We first investigate the systems with large rotational diffusivity (i.e., $D_r = 0.05$). Large D_r values correspond to rapid relaxing of the persistent velocities, which is known to diminish particle clustering in classic ABP systems. This can be clearly seen in Fig. 3 upper panels, which shows the snapshots of classic ABP system at different particle densities $\phi \in [0.1, 0.5]$ (i.e., the fraction of simulation box area covered by the particles). No significant particle clustering occurs until at very high particle density $\phi = 0.5$. On the other hand, the APPA system starts to show significant aggregation behavior at intermediate densities, e.g., $\phi = 0.3$, see Fig. 3 lower panels. The clustering behaviors of the two different systems at

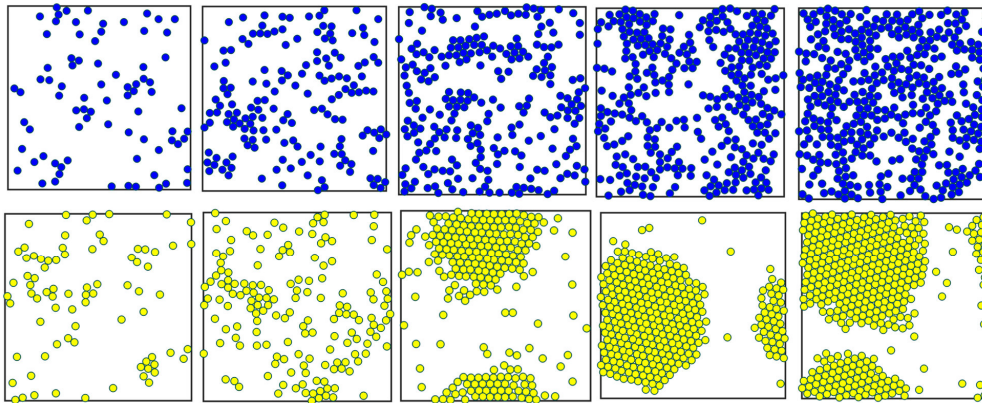


FIG. 3: Distinct aggregation behaviors at varying particle densities and large rotational diffusivity $D_r = 0.05$ rising in the classic ABP systems (upper panels) and in the APPA systems) (lower panels). The radius of the particles is $R_c = 10\mu m$ and the linear size of the periodic square simulation domain is $L = 500\mu m$. The particle densities from left to right are respectively $\phi = 0.1, 0.2, 0.3, 0.4$ and 0.5 .

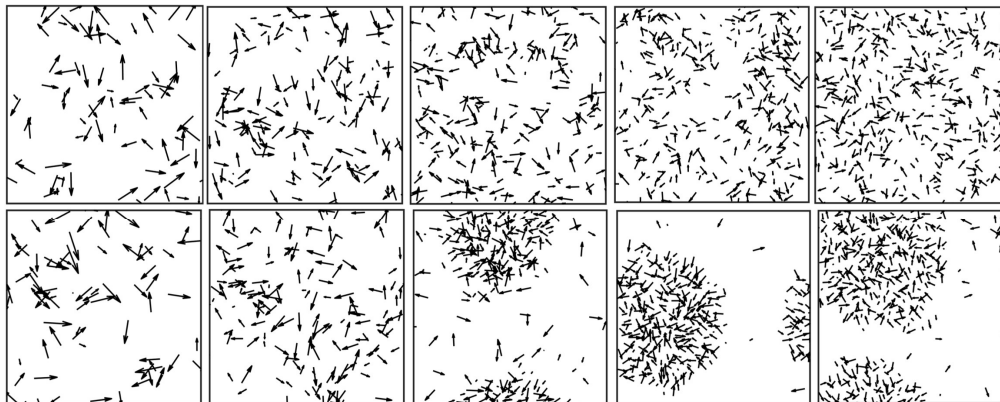


FIG. 4: Velocity maps (in which the velocity vector associated with each particle is shown as an arrow at the particle center) showing distinct velocity correlations at varying particle densities and large rotational diffusivity $D_r = 0.05$ rising in the classic ABP systems (upper panels) and in the APPA systems (lower panels). The particle densities from left to right are respectively $\phi = 0.1, 0.2, 0.3, 0.4$ and 0.5 .

varying particle densities are also quantified using time-dependent cluster statistics. Fig. 5 upper panels show the evolution of mean cluster size S (see Eq. 5 for definition) in both classic ABP system and APPA system. It can be seen that S increases rapidly in APPA system with $\phi \geq 0.3$ and asymptotically approaches unity, indicating the emergence of a dominant cluster containing majority of particles in the system.

Importantly, the APPA system exhibits distinct dynamic correlations compared to the ABP system at high particle densities. This can be clearly seen from the velocity correlation function $C(r)$ shown in Fig. 5 lower panels. It can be seen that $C(r) \approx 0$ for all r and all ϕ in the classic ABP system, regardless of the emergence of particle aggregation, indicating the particles are not dynamically correlated in the system. In contrast, the APPA system exhibits strong dynamic correlations, evidenced by the slow decaying of $C(r)$, which emerges for $\phi \geq 0.3$, coinciding with the emergence of the particle aggregation

in the corresponding system. To further understand the emergence of this dynamic correlation, we investigate the particle velocity distribution in the APPA system. Fig. 4 shows the velocity maps, in which the velocity vector associated with each particle is shown as an arrow at the particle center. It can be seen that the velocities of the particles within the dominant cluster exhibit strong local and intermediate-ranged alignment correlation. This distinct dynamics results from the effective polarized attractions in the APPA system.

We now investigate the systems with small rotational diffusivity $D_r = 0.01$. It is known that small D_r enhances the clustering in classic ABP system. Indeed, as shown in Fig. 6 upper panels, the ABP system starts to show clustering behavior at $\phi = 0.4$ and significant aggregation is observed at $\phi = 0.5$. The enhanced clustering behavior is much more significant in the APPA system, in which single dominant cluster emerges even at the lowest density $\phi = 0.1$. This is also quantified via

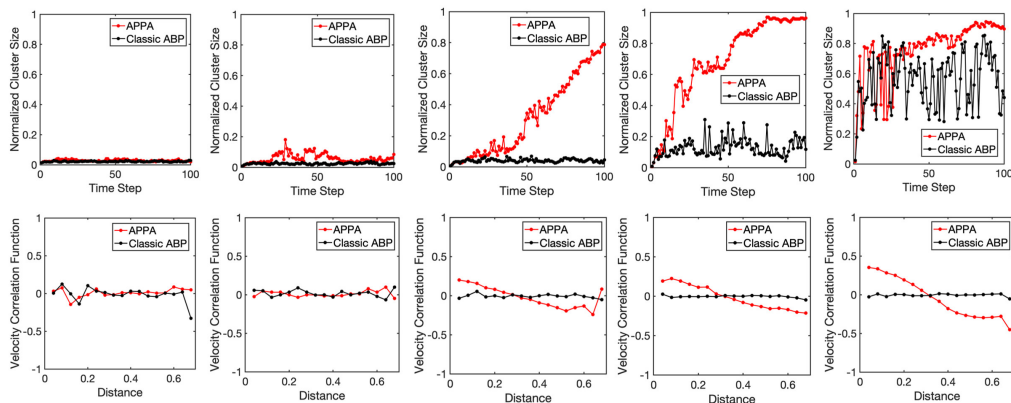


FIG. 5: Comparison of the cluster statistics S (upper panels, c.f. Eq.(5)) and velocity correlation functions $C(r)$ (lower panels, c.f. Eq.(6)) associated with the classic ABP systems and the APPA systems at large rotational diffusivity $D_r = 0.05$ and varying particle densities. The particle densities from left to right are respectively $\phi = 0.1, 0.2, 0.3, 0.4$ and 0.5 . The unit of distance is given by the length of the square simulation box.

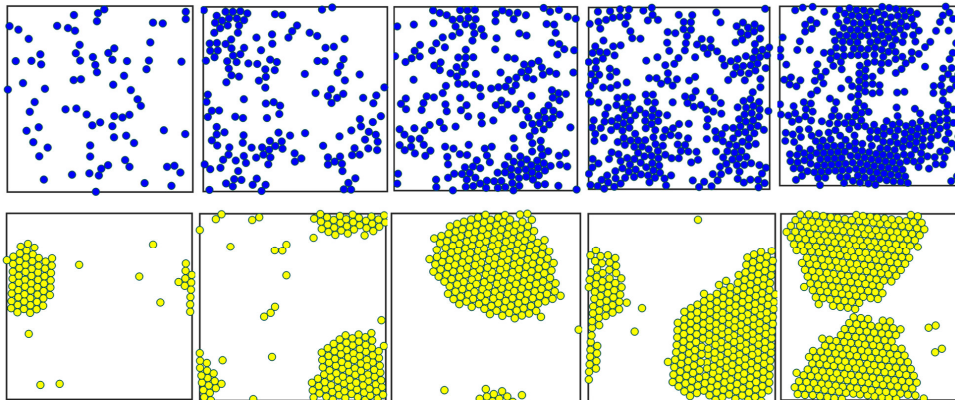


FIG. 6: Distinct aggregation behaviors at varying particle densities and small rotational diffusivity $D_r = 0.01$ rising in the classic ABP systems (upper panels) and in the APPA systems) (lower panels). The radius of the particles is $R_c = 10\mu m$ and the linear size of the periodic square simulation domain is $L = 500\mu m$. The particle densities from left to right are respectively $\phi = 0.1, 0.2, 0.3, 0.4$ and 0.5 .

the time-dependent mean cluster size S shown in Fig. 8 upper panels. Moreover, strong dynamic correlations are observed in the APPA system for all particle densities $\phi \in [0.1, 0.5]$, which is consistent with the emergence of particle clusters at low densities. The dynamic correlations can be clearly seen in the velocity maps (see Fig. 7) and the corresponding slow decay in the velocity correlation functions $C(r)$ shown in Fig. 8 lower panels.

These results indicate that the polarized effective attraction mimicking the influence of mechanical dialog among the cells can lead to significantly enhanced dynamics correlations among particles, especially at lower particle densities and larger rotational diffusivity. In the next section, we test these model predictions using *in vitro* experiments.

B. Experimental verification via MCF-10A cells on 3D collagen gel

To test the predictions of APPA model, we observe *in vitro* the migration of multiple MCF-10A cells on 3D collagen I hydrogel with a collagen concentration $2mg/ml$. Single cell migration dynamics is acquired by recording and analyzing cell trajectories after 12-hours culture. The fibrous microstructure of collagen gels can support long-range force propagation, which is crucial to mechanical signaling among the cells. MCF-10A cells are selected because these cells possess relatively high motility on top of the collagen gel, but are not able to invade into the gel. On the other hand, the strong motility of the MCF-10A cells can generate significant contractile forces during migration, and thus potentially induce strong cell-ECM mechanical coupling. Additional details of the experimental studies are reported elsewhere [40].

In particular, we randomly distribute the MCF-10A

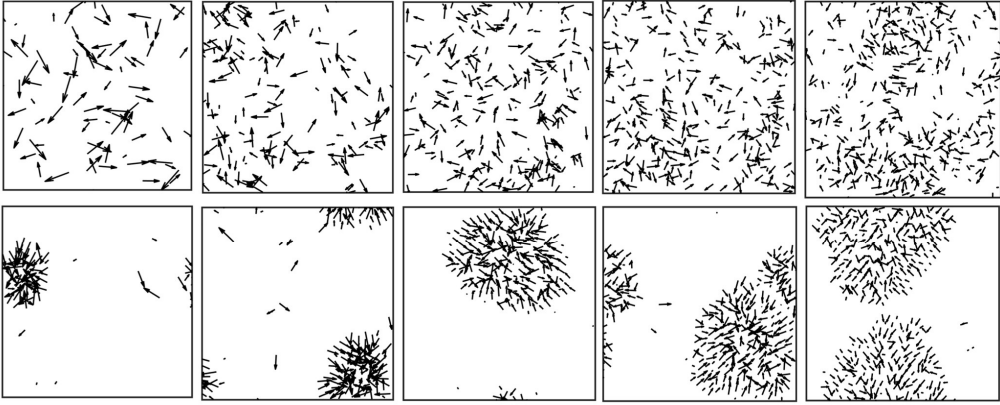


FIG. 7: Velocity maps (in which the velocity vector associated with each particle is shown as an arrow at the particle center) showing distinct velocity correlations at varying particle densities and small rotational diffusivity $D_r = 0.01$ rising in the classic ABP systems (upper panels) and in the APPA systems (lower panels). The particle densities from left to right are respectively $\phi = 0.1, 0.2, 0.3, 0.4$ and 0.5 .

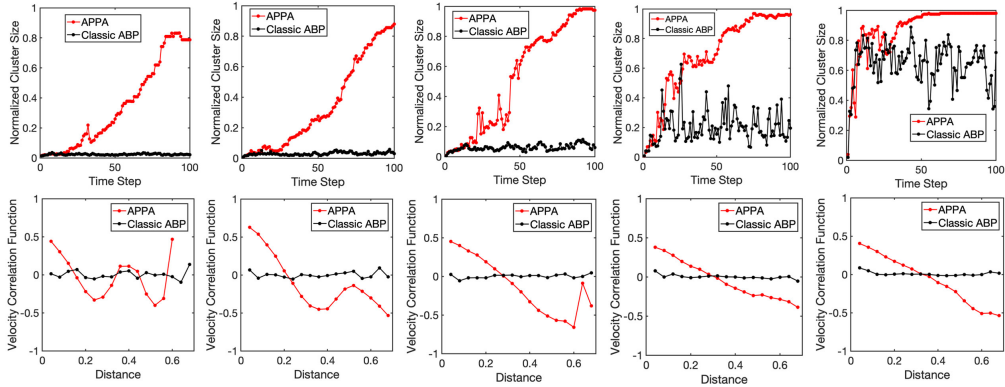


FIG. 8: Comparison of the cluster statistics S (upper panels, c.f. Eq.(5)) and velocity correlation functions $C(r)$ (lower panels, c.f. Eq.(6)) associated with the classic ABP systems and the APPA systems at small rotational diffusivity $D_r = 0.01$ and varying particle densities. The particle densities from left to right are respectively $\phi = 0.1, 0.2, 0.3, 0.4$ and 0.5 . The unit of distance is given by the length of the square simulation box.

cells on collagen-based ECM with two distinct cell density, corresponding to the simulation values (i.e., $\phi \approx 0.1$ and 0.5). We observe rapid and strong aggregation in the high-density system while the cells in the low-density system remain separated (see Fig. 9a and b). We also compute the cluster statistics S (Fig. 9c) as well as the velocity correlation functions $C(r)$ (Fig. 9d), based on the trajectory data via cell tracking [40]. Consistent with the simulation results, the cells within the cluster in the high-density system exhibit strong dynamic correlations, as indicated by the long-range slowly-decaying $C(r)$, as well as the strong centripetal migration dynamics. The cells in the low-density system are largely uncorrelated, evidenced by the flat velocity correlation function and the random cell motions.

C. Phase diagram of active particles with polarized attractions

The results in previous sections indicate that the polarized effective attractions may play an important role in giving rise to unique collective dynamics in multi-cellular systems (such as the strong dynamic correlation within cell aggregates). In an actual multi-cell-ECM system, the cell phenotype, ECM microstructure and physical properties can all affect the active force transmission, and thus, the effective attraction in our model. In this section, we systematically vary the key model parameter δ [c.f. Eq. (4)] that determines the “region of influence” of the polarized forces and investigate its effects on the overall aggregation behavior and collective dynamics of the system.

In particular, for each δ , we map the observed collective behaviors of the APPA system at different rotational diffusivity D_r and particle density ϕ to a “phase dia-

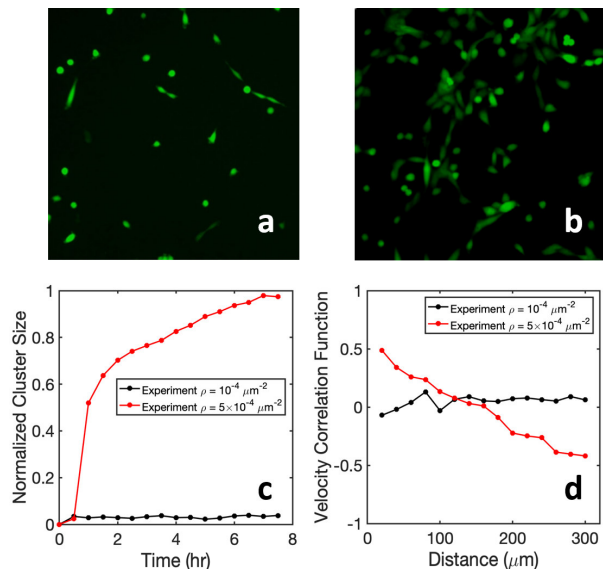


FIG. 9: Verification of the predicted enhanced aggregation and dynamic correlation in APPA system using *in vitro* experiments of MCF-10A cells on 3D collagen gels. Panel (a) and (b) respectively shows snapshots of arrangements of the cells at $\phi \approx 0.1$ and 0.5 at approximately 6 hours after initial seeding. The linear size of the image shown here is $\sim 500\mu\text{m}$. Panel (c) shows the evolution of the mean cluster size S which clearly indicates aggregation behavior at high cellular density. Panel (d) shows the velocity correlation function $C(r)$, where the slower decay at high cellular density indicates the stronger correlated dynamics resulted from the collective centripetal migration mode.

gram”, where the aggregation/clustering phase and dispersion/scattered phase are distinguished. Note that the particles in the aggregation phase also possess strong dynamic correlations. Figure 10 shows the phase diagrams of the APPA system for varying δ , D_r and ϕ . For a given δ , the aggregation phase emerges at relatively small D_r and large ϕ . We note that the classic ABP model can be obtained by setting $\delta = 0$. By increasing δ , i.e., force influence region, the aggregation-dispersion phase boundary is pushed to larger D_r and smaller ϕ , indicating enhanced aggregation behaviors due to mechanical communication. We note that the largest δ considered here corresponds to a mis-alignment angle tolerance of $\pi/20$, which is still relatively small.

IV. CONCLUSIONS AND DISCUSSION

Motivated by recent experimental evidence that ECM-mediate mechanical coupling among migration cells regulates their collective dynamics, we develop an active-particle model with polarized effective attractions (APPA), which generalizes the classic active-Brownian-particle (ABP) model. Specifically, in the APPA model, pairwise polarized attractive forces are imposed between

the particles moving towards one another, which mimics the effective mutual pulling between the cells via the fiber bundle bridge. The APPA system exhibits enhanced aggregation behaviors compared to classic ABP system, especially at lower particle densities ϕ and larger rotational diffusivities D_r . Importantly, in contrast to the classic ABP system where the particle velocities are not correlated for all particle densities, the high-density phase of APPA system exhibits strong dynamic correlation, which is characterized by the slowly decaying velocity correlation functions $C(r)$ with a correlation length comparable to the linear size of high-density phase domain (i.e., cluster of the particles).

We validate our model by accurately reproducing collective dynamics of MCF-10A breast cancer cells migrating on 3D collagen gels, including enhanced aggregation behaviors. Moreover, our model predicts strongly correlated multi-cellular migration dynamics, which are resulted from the ECM-mediated mechanical coupling among the migrating cells and also verified in *in vitro* experiments using MCF-10A cells. Our studies indicate the importance of incorporating ECM-mediated mechanical coupling among the migrating cells for appropriately modeling emergent multi-cellular dynamics in complex micro-environments.

Although currently focusing on 2D multi-cellular systems (e.g., non-metastatic MCF-10A breast cancer cells migrating on top of 3D ECM), our model can be easily generalize to investigate the migration of mesenchymal cells (e.g., invasive MDA-MB-231 breast cancer cells) in 3D ECM. The key modification is to explicitly incorporate the effects of ECM degradation by the cells, which leads to micro-channels that bias cell migration in addition to the ECM-mediated mechanical coupling. In addition, the effects of chemotaxis and cell-cell adhesion can also be incorporated into the model to investigate a wide range of cell lines with different phenotypes. With proper modifications and generalizations, as well as efficient parallel implementations, it is expected that the model could be employed to investigate collective migratory behaviors and emergent self-organizing multi-cellular patterns resulted from ECM-mediated mechanical signaling among the cells.

Acknowledgments

The authors are extremely grateful to the anonymous reviewers. Y. Z. and Y. J. thank Arizona State University for the generous start-up funds and the University Graduate Fellowships. Q. F., X. W., and F. Y. thank the support of the National Natural Science Foundation of China (Grant Nos. 11704404, 11774394) and the Key Research Program of Frontier Sciences of Chinese Academy of Sciences (Grant No. QYZDB-SSW-SYS003). C. Z. E and B. S. thank the support from the National Science Foundation Grant PHY-1400968.

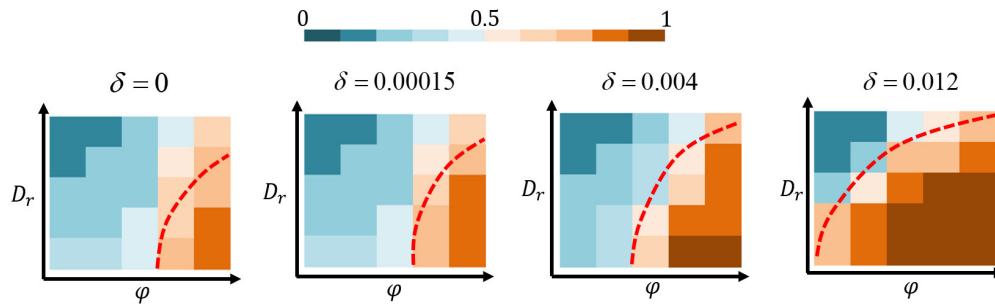


FIG. 10: Phase diagrams of the APPA system for varying δ , D_r and ϕ . Each diagram is associated with a fixed δ , and collective behaviors of the APPA system at different rotational diffusivity $D_r \in [0.01, 0.2]$ and particle density $\phi \in [0.1, 0.5]$ are mapped to two distinct phase regions, i.e., the aggregation/clustering phase and dispersion/scattered phase. The colors indicate the values of mean cluster size S . Increasing δ (i.e., the region of influence of the polarized attractions) leads to enhanced aggregation/clustering behavior and thus, stronger dynamic correlation in the aggregation phase. From the left to the right, $\delta = 0, 0.00015, 0.004$ and 0.012 , respectively corresponding to mis-alignment angle tolerance of $0, \pi/180, \pi/36$ and $\pi/20$. We note that the classic ABP model is associated with $\delta = 0$.

-
- [1] A. J. Ridley, M.A. Schwartz, K. Burridge, R.A. Firtel, M.H. Ginsberg, G. Borisy, J.T. Parsons, and A.R. Horwitz, Cell migration: integrating signals from front to back. *Science* **302**, 1704-1709 (2003).
- [2] P. Friedl, and E.-B. Brocker, The biology of cell locomotion within three-dimensional extracellular matrix. *Cellular and Molecular Life Sciences* **57**, 41-64 (2000).
- [3] A. Aman, and T. Piotrowski, Cell migration during morphogenesis. *Developmental Biology* **341**, 20-33 (2010)
- [4] P. Friedl, and D. Gilmour, Collective cell migration in morphogenesis, regeneration and cancer. *Nature Reviews Molecular Cell Biology* **10**, 445 (2009).
- [5] A. Vaezi, C. Bauer, V. Vasioukhin, and E. Fuchs, Actin cable dynamics and Rho/Rock orchestrate a polarized cytoskeletal architecture in the early steps of assembling a stratified epithelium. *Developmental Cell* **3**, 367-381 (2002).
- [6] S. Werner, T. Krieg, and H. Smola, Keratinocytefibroblast interactions in wound healing. *Journal of Investigative Dermatology* **127**, 998-1008 (2007).
- [7] H. Szurmant, and G.W. Ordal, Diversity in chemotaxis mechanisms among the bacteria and archaea. *Microbiology and Molecular Biology Reviews* **68**, 301-319 (2004).
- [8] S. V. Plotnikov, A.M. Pasapera, B. Sabass, and C.M. Waterman, Force fluctuations within focal adhesions mediate ECM-rigidity sensing to guide directed cell migration. *Cell* **151**, 1513-1527 (2012).
- [9] R. Sunyer, V. Conte, J. Escribano, A. Elosegui-Artola, A. Labernadie, L. Valon, D. Navajas, J.M. Garca-Aznar, J.J. Munoz, and P. Roca-Cusachs, Collective cell durotaxis emerges from long-range intercellular force transmission. *Science* **353**, 1157-1161 (2016).
- [10] E. Hadjipanayi, V. Mudera, and R. A. Brown, Guiding cell migration in 3D: a collagen matrix with graded directional stiffness. *Cell Motil. Cytoskeleton* **66** 121-8 (2009).
- [11] S. B. Carter, Haptotaxis and the mechanism of cell motility. *Nature* **213**, 256 (1967).
- [12] P. P. Provenzano, D.R. Inman, K.W. Eliceiri, S.M. Trier, and P.J. Keely, Contact guidance mediated three-dimensional cell migration is regulated by Rho/ROCK-dependent matrix reorganization. *Biophysical Journal* **95**, 5374-5384 (2008).
- [13] J. H. Wang, and E.S. Grood, The strain magnitude and contact guidance determine orientation response of fibroblasts to cyclic substrate strains. *Connective Tissue Research* **41**, 29-36 (2000).
- [14] S. Guido and R. T. Tranquillo, A methodology for the systematic and quantitative study of cell contact guidance in oriented collagen gels. Correlation of fibroblast orientation and gel birefringence. *J. Cell Sci.* **105**, 317-31 (1993).
- [15] R. Ananthakrishnan, and A. Ehrlicher, The Forces Behind Cell Movement, *Int. J. Biol. Sci.* **3**, 303317 (2007).
- [16] M. J. Footer, J. W. J. Kerssemakers, J. A. Theriot, and M. Dogterom, Direct measurement of force generation by actin filament polymerization using an optical trap, *Proceedings of the National Academy of Sciences* **104**, 2181-2186 (2007).
- [17] S. Wang, and P.G. Wolynes, Active contractility in actomyosin networks. *Proceedings of the National Academy of Sciences* **109**, 6446-6451 (2012).
- [18] T. Lecuit, P.-F. Lenne, and E. Munro, Force generation, transmission, and integration during cell and tissue morphogenesis. *Annual Review of Cell and Developmental Biology* **27**, 157-184 (2011).
- [19] M. A. Schwartz, Integrins and extracellular matrix in mechanotransduction. *Cold Spring Harbor perspectives in biology*, a005066 (2010).
- [20] G. Totsukawa, Y. Wu, Y. Sasaki, D.J. Hartshorne, Y. Yamakita, S. Yamashiro, and F. Matsumura, Distinct roles of MLCK and ROCK in the regulation of membrane protrusions and focal adhesion dynamics during cell migration of fibroblasts. *The Journal of Cell Biology* **164**, 427-439 (2004).
- [21] C. A. Jones, M. Cibula, J. Feng, E.A. Krnacik, D.H. McIntyre, H. Levine, and B. Sun, Micromechanics of cellularized biopolymer networks. *Proceedings of the National Academy of Sciences* **112**, E5117-E5122 (2015).

- [22] S. B. Lindstrom, D.A. Vader, A. Kulachenko, and D.A. Weitz, Biopolymer network geometries: characterization, regeneration, and elastic properties. *Physical Review E* **82**, 051905 (2010).
- [23] H. Mohammadi, P.D. Arora, C.A. Simmons, P.A. Janmey, and C.A. McCulloch, Inelastic behaviour of collagen networks in cellmatrix interactions and mechanosensation. *Journal of The Royal Society Interface* **12**, 20141074 (2015).
- [24] S. Nam, K.H. Hu, M.J. Butte, and O. Chaudhuri, Strain-enhanced stress relaxation impacts nonlinear elasticity in collagen gels. *Proceedings of the National Academy of Sciences*, 201523906 (2016).
- [25] Nam, S., J. Lee, D.G. Brownfield, and O. Chaudhuri, Viscoplasticity enables mechanical remodeling of matrix by cells. *Biophysical journal*, 2016. 111(10): p. 2296-2308.
- [26] J. Kim, J. Feng, C.A. Jones, X. Mao, L.M. Sander, H. Levine, and B. Sun, Stress-induced plasticity of dynamic collagen networks. *Nature Communications* **8**, 842 (2017).
- [27] S. Chen, W. Xu, J. Kim, H. Nan, Y. Zheng, B. Sun, and Y. Jiao, Novel inverse finite-element formulation for reconstruction of relative local stiffness in heterogeneous extra-cellular matrix and traction forces on active cells. *Physical Biology* **16**, 036002 (2019).
- [28] A. D. Doyle, N. Carvajal, A. Jin, K. Matsumoto, and K.M. Yamada, Local 3D matrix microenvironment regulates cell migration through spatiotemporal dynamics of contractility-dependent adhesions. *Nature Communications* **6**, 8720 (2015).
- [29] F. Grinnell, and W.M. Petroll, Cell motility and mechanics in three-dimensional collagen matrices. *Annual Review of Cell and Developmental Biology* **26**, 335-361 (2010).
- [30] Y. L. Han, P. Ronceray, G. Xu, A. Malandrino, R.D. Kamm, M. Lenz, C.P. Broedersz, and M. Guo, Cell contraction induces long-ranged stress stiffening in the extracellular matrix. *Proceedings of the National Academy of Sciences* **115**, 4075-4080 (2018).
- [31] X. Ma, M.E. Schickel, M.D. Stevenson, A.L. Sarang-Sieminski, K.J. Gooch, S.N. Ghadiali, and R.T. Hart, Fibers in the extracellular matrix enable long-range stress transmission between cells. *Biophysical Journal* **104**, 1410-1418 (2013).
- [32] P. Ronceray, C.P. Broedersz, and M. Lenz, Fiber networks amplify active stress. *Proceedings of the National Academy of Sciences* **113**, 2827-2832 (2016).
- [33] H. Wang, A. Abhilash, C.S. Chen, R.G. Wells, and V.B. Shenoy, Long-range force transmission in fibrous matrices enabled by tension-driven alignment of fibers. *Biophysical Journal* **107**, 2592-2603 (2014).
- [34] F. Beroz, L.M. Jawerth, S. Munster, D.A. Weitz, C.P. Broedersz, and N.S. Wingreen, Physical limits to biomechanical sensing in disordered fibre networks. *Nature Communications* **8**, 16096 (2017).
- [35] L. Liang, C. Jones, S. Chen, B. Sun, and Y. Jiao, Heterogeneous force network in 3D cellularized collagen networks. *Physical Biology* **13**, 066001 (2016).
- [36] H. Nan, Y. Zheng, Y. H. Lin, S. Chen, C. Z. Eddy, J. Tian, W. Xu, B. Sun, and Y. Jiao, Absorbing-Active Transition in Multi-Cellular System Regulated by Dynamic Force Network, *Soft Matter* **15**, 6938 (2019).
- [37] A. A. Alobaidi, Y. Xu, Y. Jiao, B. Sun, Probing Cooperative Force Generation in Collective Cancer Invasion, *Physical Biology* **14**, 045005 (2017).
- [38] Y. Zheng, H. Nan, Y. Liu, Q. Fan, X. Wang, R. Liu, L. Liu, F. Ye, B. Sun, and Y. Jiao, Modeling Cell Migration Regulated by Cell-ECM Micromechanical Coupling, *Physical Review E* **100**, 043303 (2019)
- [39] J. Kim, Y. Zheng, A. A. Alobaidi, H. Nan, J. Tian, Y. Jiao, and B. Sun, Geometric Dependence of Three-Dimensional Collective Cancer Invasion, *Biophysical Journal* **118**, 1177 (2020)
- [40] Q. Fan, Y. Zheng, Y. Jiao, and F. Ye, Strongly correlated cell dynamics induced by ECM-mediated long-range mechanical coupling, submitted.
- [41] M. H. Zaman, R. D. Kamm, P. Matsudaria, and D. A. Lauffenburger. Computational model for cell migration in three-dimensional matrices. *Biophys. J.* **89**, 1389 (2005).
- [42] A. Vaziri and A. Gopinath. Cell and biomolecular mechanics in silico. *Nature Materials* **7**, 15 (2008).
- [43] P. Masuzzo, M. Van Troys, C. Ampe, and L. Martens, Taking aim at moving targets in computational cell migration. *Trends in cell biology* **26**, 88 (2016).
- [44] F. Ziebert, S. Swaminathan, and I. S. Aranson. Modeling for self-polarization and motility of keratocyte fragments. *J. R. Soc. Interface* **9**, 1084 (2011).
- [45] D. Shao, W. J. Rappel, and H. Levine. Computational model for cell morphodynamics. *Phys. Rev. Lett.* **105**, 108104 (2010).
- [46] D. Shao, H. Levine, and W. J. Rappel. Coupling actin flow, adhesion, and morphology in a computational cell motility model. *Proc. Natl. Acad. Sci. USA* **109**, 6851 (2012).
- [47] U. Z. George, A. Stephanou, and A. Madzvamuse. Mathematical modeling and numerical simulations of actin dynamics in the eukaryotic cell. *J. Math. Biol.* **66**, 547 (2013).
- [48] T. C. Bidone, W. Jung, D. Maruri, C. Borau, R. D. Kamm, and T. Kim, Morphological transformation and force generation of active cytoskeletal networks, *PLoS Comput. Biol.* **13**, e1005277 (2017).
- [49] M. C. Kim, J. Whisler, Y. R., Silberberg, et al. Cell invasion dynamics into a three dimensional extracellular matrix fibre network. *PLoS Comput. Biol.* **11**, e1004535 (2015).
- [50] T. Vicsek, A. Czirok, E. Ben-Jacob, I. Cohen, and O. Shochet, Novel type of phase transition in a system of self-driven particles. *Physical review letters* **75**, 1226 (1995).
- [51] C. Bechinger, R. Di Leonardo, H. Lowen, C. Reichhardt, G. Volpe, Active particles in complex and crowded environments. *Reviews of Modern Physics* **88**, 045006 (2016).
- [52] D. Bi, J. Lopez, J. Schwarz, M. L. Manning, A density-independent rigidity transition in biological tissues, *Nature Physics* **11**, 1074 (2015).
- [53] F. Graner, and J. A. Glazier, Simulation of biological cell sorting using a two-dimensional extended Potts model. *Physical Review Letters* **69**, 2031 (1992).
- [54] Y. Jiao and S. Torquato, Emergent Properties from a Cellular Automaton Model for Invasive Tumor Growth in Heterogeneous Environment, *PLoS Computational Biology* **7**, 1002314 (2011).
- [55] Y. Jiao and S. Torquato, Diversity of Dynamics and Morphologies of Invasive Solid Tumors, *AIP Advances* **2**, 011003 (2012)
- [56] Y. Jiao and S. Torquato, Evolution and Morphology of Microenvironment-Enhanced Malignancy of Three-

- Dimensional Invasive Solid Tumors, *Physical Review E* **87**, 052707 (2013)
- [57] H. Xie, Y. Jiao, Q. Fan, et. al., Modeling Three-dimensional Invasive Solid Tumor Growth in Heterogeneous Microenvironment under Chemotherapy, *PLoS One* **13**, e0206292 (2018)
- [58] Jakob Lober, Falko Ziebert and Igor S. Aranson, Modeling crawling cell movement on soft engineered substrates, *Soft Matter* **10**, 1365-1373 (2014)
- [59] Jakob Lober, Falko Ziebert, and Igor S. Aranson, Collisions of deformable cells lead to collective migration, *Sci Rep.* **5**: 9172 (2015).
- [60] Andriy Goychuk, David B. Bruckner, Andrew W. Holle, Joachim P. Spatz, Chase P. Broedersz, Erwin Frey, Morphology and Motility of Cells on Soft Substrates arXiv:1808.00314 (2018)
- [61] Zhu J., and Mogilner A., Comparison of cell migration mechanical strategies in three-dimensional matrices: a computational study, *Interface Focus* **6**, 20160040 (2016).
- [62] A. Moure, H. Gomez, Phase-field model of cellular migration: Three-dimensional simulations in fibrous networks, *Computer Methods in Applied Mechanics and Engineering* **320**, 162-197 (2017).
- [63] A. Moure, H. Gomez, Three-dimensional simulation of obstacle-mediated chemotaxis, *Biomechanics and Modeling in Mechanobiology* **17**, 1243-1268 (2018).
- [64] H. Abdel-Rahman, B. Thomas, and T. Kim, A mechanical model for durotactic cell migration, *ACS Biomater Sci Eng* (2019)
- [65] M. Dietrich, H. Le Roy, D. B. Bruckner, H. Engelke, R. Zantl, J. O. Radler and C. P. Broedersz, Guiding 3D cell migration in deformed synthetic hydrogel microstructures, *Soft Matter* **14**, 2816 (2018).
- [66] Staddon, M. F. , Bi, D. , Tabatabai, A. P. , Ajeti, V. , Murrell, M. P. , Banerjee, S. , et al. (2018). Cooperation of dual modes of cell motility promotes epithelial stress relaxation to accelerate wound healing. *PLoS Computational Biology*, 14(10).
- [67] Visar Ajeti, A. Pasha Tabatabai, Andrew J. Fleszar, Michael F. Staddon, Daniel S. Seara, Cristian Suarez, M. Sulaiman Yousafzai, Dapeng Bi, David R. Kovar, Shiladitya Banerjee and Michael P. Murrell, Wound healing coordinates actin architectures to regulate mechanical work, *Nature Physics* (2019).
- [68] E. N. Schaumanna, M. F. Staddon, M. L. Gardel, and S. Banerjee, Force localization modes in dynamic epithelial colonies, *Molecular Biology of the Cell* **29**, 2835 (2018).
- [69] J. Feng, H. Levine, X. Mao, et. al., Stiffness sensing and cell motility: Durotaxis and contact guidance, *Soft Matter*, 2019.
- [70] J. M. Belmonte, G. L. Thomas, L. G. Brunnet, et. al. Self-Propelled Particle Model for Cell-Sorting Phenomena, *Phys. Rev. Lett.* **100**, 248702 (2008).
- [71] X. Yang, M. L. Manning, M. C. Marchetti, Aggregation and segregation of confined active particles, *Soft matter* **10**, 6477 (2014).
- [72] R. Ni, M. A. Cohen Stuart, P. G. Bolhuis, Tunable long range forces mediated by self-propelled colloidal hard spheres, *Physical Review Letters* **114**, 018302 (2015).
- [73] Z. Preisler and M. Dijkstra, Configurational entropy and effective temperature in systems of active Brownian particles, *Soft Matter* **12**, 6043 (2016).
- [74] Nan, H., L. Liang, G. Chen, L. Liu, R. Liu, and Y. Jiao, Realizations of highly heterogeneous collagen networks via stochastic reconstruction for micromechanical analysis of tumor cell invasion. *Physical Review E* **97**, 033311 (2018).
- [75] C. Jones, L. Liang, D. Lin, Y. Jiao, and B. Sun, The Spatial-Temporal Characteristics of Type I Collagen-Based Extracellular Matrix, *Soft Matter* **10**, 8855 (2014).
- [76] S. Kirkpatrick, C. D. Gelatt, and M. P. Vecchi, Optimization by simulated annealing. *Science* **220**, 671 (1983).
- [77] D. A. Head, A. J. Levine, and F. C. MacKintosh, Mechanical response of semiflexible networks to localized perturbations. *Phys. Rev. E* **72** 061914 (2005).
- [78] Y. Shokef and S. A. Safran, Scaling laws for the response of nonlinear elastic media with implications for cell mechanics. *Phys. Rev. Lett.* **108**, 178103 (2012).
- [79] J. Steinwachs, C. Metzner, K. Skodzek, et. al. Three-dimensional force microscopy of cells in biopolymer networks. *Nat. Method* **13** 171-6 (2016).
- [80] C. Heussinger and E. Frey, Force distributions and force chains in random stiff fiber networks. *Eur. Phys. J. E* **24** 4753 (2007).
- [81] Burkel, B., Proestaki, M., Tyznik, S., and Notbohm, J. Heterogeneity and nonaffinity of cell-induced matrix displacements. *Phys Rev E* **98**, 052410 (2018).
- [82] S Tyznik, J Notbohm, Length Scale Dependent Elasticity in Random Three-Dimensional Fiber Networks, *Mechanics of Materials*, (2019).
- [83] S. Torquato and Y. Jiao, Effect of Dimensionality on the Continuum Percolation of Overlapping Hyperspheres and Hypercubes. II. Simulations and Analyses, *Journal of Chemical Physics* **137**, 074106 (2012)
- [84] S. Torquato and Y. Jiao, Effect of Dimensionality on the Percolation Threshold of Anisotropic Overlapping Particles, *Physical Review E* **87**, 022111 (2013)
- [85] S. Torquato and Y. Jiao, Effect of Dimensionality on the Percolation Thresholds of Various d-Dimensional Lattices, *Physical Review E* **87**, 032149 (2013)